SPANDIDOS PUBLICATIONS

MOLECULAR MEDICINE REPORTS 20: 584-592, 2019

iTRAQ-based proteomic analysis of endotoxin tolerance induced by lipopolysaccharide

QIAN ZHANG[1], YINGCHUN HU[2], JING ZHANG[1] and CUNLIANG DENG[1]

Departments of [1]Infectious Diseases and [2]Emergency,
The Affiliated Hospital of Southwest Medical University, Luzhou, Sichuan 646000, P.R. China

Received August 25, 2018; Accepted February 15, 2019

DOI: 10.3892/mmr.2019.10264

Abstract. The purpose of the present study was to investigate the differentially expressed proteins between endotoxin tolerance and sepsis. Cell models of an endotoxin tolerance group (ET group) and sepsis group [lipopolysaccharide (LPS) group] were established using LPS and evaluated using ELISA and flow cytometry methods. Differentially expressed proteins between the ET and the LPS groups were identified using isobaric tags for relative and absolute quantitation (iTRAQ) analysis and evaluated by bioinformatics analysis. The expression of core proteins was detected by western blotting. It was identified that the expression of tumor necrosis factor-α and interleukin-6 was significantly decreased in the ET group compared with the LPS group. Following high-dose LPS stimulation for 24 h, the positive rate of cluster of differentiation-16/32 in the ET group (79.07%) was lower when compared with that of the LPS group (94.27%; $P<0.05$). A total of 235 proteins were identified by iTRAQ, and 36 upregulated proteins with >1.2-fold differences and 27 downregulated proteins with <0.833-fold differences were detected between the ET and LPS groups. Furthermore, the expression of high mobility group (HMG)-A1 and HMGA2 in the ET group was higher compared with the LPS group following high-dose LPS stimulation for 4 h, while HMGB1 and HMGB2 exhibited the opposite expression trend under the same conditions. In conclusion, proteomics analysis using iTRAQ technology contributes to a deeper understanding of ET mechanisms. HMGA1, HMGA2, HMGB1 and HMGB2 may serve a crucial role in the development of ET.

Correspondence to: Dr Cunliang Deng, Department of Infectious Diseases, The Affiliated Hospital of Southwest Medical University, 25 Taiping Street, Jiangyang, Luzhou, Sichuan 646000, P.R. China
E-mail: 782872184@qq.com

Key words: endotoxin tolerance, isobaric tags for relative and absolute quantitation, sepsis, proteomics, bioinformatics

Introduction

Sepsis is a serious healthcare concern due to its high costs and mortality rate (1). It is triggered mainly by Gram-negative bacteria (2) and lipopolysaccharides (LPS) are the main component of the outer membrane of Gram-negative bacteria. Previous studies have demonstrated that LPS serve an important role in sepsis, and can stimulate the mononuclear phagocytic system to produce a large number of inflammatory factors and cause systemic inflammatory response, sepsis, infectious shock and multiple organ dysfunctions (3). It has been reported that following low-dose LPS stimulation, the host can survive a second lethal dose of LPS treatment, indicating a phenomenon known as endotoxin tolerance (ET) (4). ET is characterized as the reduced capacity of a cell or organ to respond to LPS stimulation after an initial exposure to endotoxin (5,6), and it is an adaptive host response as a self-protective regulatory mechanism of the body (7). The main characteristics of ET are downregulation of inflammatory factors including tumor necrosis factor (TNF)-α, interleukin (IL)-6, and upregulation of anti-inflammatory mediators such as IL-10 (8). Macrophages serve an important role in innate and acquired immunity, with ET representing an M2-like phenotype, and the characteristic cell surface markers cluster of differentiation (CD)206 and CD163 of the macrophages are significantly induced, and the genes associated with phagocytosis also were markedly upregulated (9). A previous study demonstrated that LPS significantly induced the apoptosis of immune cells to prevent hypernomic inflammation in patients with sepsis, and T-cell and B-cell deficient mice were more likely to develop ET than wild-type mice (10). Previous studies have identified that the Toll-like receptor (TLR)-4 pathway is involved in the formation of ET (6,11). Toll interacting protein (Tollip), as a negative regulator of TLR4 signaling pathway, which complexes with IL-1 receptor-associated kinase (IRAK) and suppressed activation of IRAK as molecular hallmarks of ET, were shown to have increased expression in ET (12). ET inhibited the phosphorylation of extracellular signal-regulated kinases 1/2 (ERK1/2), Jun N-terminal kinases (JNK), and showed decreased expression of P38MAPK (13) .miRNAs regulate inflammatory factors and mediate ET through binding to mRNA or acting on the relevant members of the TLRs pathway (14). miR-146 is significant for LPS-induced tolerance and may be the most important miRNA in ET (15).

It has been reported that miR-146 negatively regulated the TLRs pathway by repressing the expression of IRAK1 and TNF receptor associated factor 6 (TRAF6), thereby resulting in ET (16,17).

Although ET has been extensively studied, its mechanism remains unclear. A previous study suggested that almost all sepsis gene expression is closely associated with ET signaling, and these signals may serve an important role in predicting organ damage and the prognosis of patients with sepsis (18). Few comprehensive studies on ET-associated proteins have been reported; thus, the present study focused on protein complexes. In the present study, proteomics analysis using isobaric tags for relative and absolute quantitation (iTRAQ) was performed to explore the mechanism of ET, and key proteins were analyzed by bioinformatics analysis.

Materials and methods

Cell culture and ET cell model establishment. Mouse macrophage RAW264.7 cells (American Type Culture Collection, Manassas, VA, USA) were cultured in Dulbecco's modified Eagle's medium (DMEM; Hyclone; GE Healthcare Life Sciences, Logan, UT, USA) containing 10% fetal bovine serum (FBS; Hyclone; GE Healthcare Life Sciences) at 37˚C in incubator with 5% CO_2. The ET group was cultured as follows: RAW264.7 cells ($5x10^5$/ml) were cultured in DMEM containing 10 ng/ml LPS (Sigma-Aldrich; Merck KGaA) at 37˚C for 24 h, followed by 100 ng/ml LPS for 4 h at 37˚C. The LPS group was cultured as follows: RAW264.7 ($5x10^5$/ml) cells were cultured in DMEM with 100 ng/ml LPS for 4 h at 37˚C. Subsequently, the RAW264.7 cells of the 2 groups were harvested for analysis.

Enzyme-linked immunosorbent assays (ELISAs). The concentration of tumor necrosis factor (TNF)-α, interleukin (IL)-6 and IL-10 in the cell supernatant of the ET and LPS groups was measured using ELISA kits (TNF-α, cat. no. EK0527; IL-6, cat. no EK0411; IL-10, cat. no. EK04167; Wuhan Boster Biological Technology, Ltd.) according to the manufacturer's instructions. The assay was performed in triplicate, and the absorbance in each well was measured with a microplate reader at 450 nm.

Flow cytometric analysis. RAW264.7 cells in the ET and LPS groups were treated with 100 ng/ml LPS for 4 or 24 h as aforementioned, then washed twice with PBS and centrifuged at 1,000 x g for 3 min at room temperature. The cell precipitate was resuspended in PBS and adjusted to a concentration of $1x10^6$/ml. Cells were stained with fluorescein isothiocyanate tagged monoclonal anti-CD-16/32 kit (cat. no. 561728, BD Biosciences Pharmingen), diluted with PBS, for 30 min at room temperature in the dark in accordance with the manufacturer's protocol, then washed two times with PBS and resuspended in PBS. Analysis was performed using the BD FACSVerse system flow cytometer and BD FACSuite version 1.0 software (BD Biosciences).

iTRAQ proteomics analysis. Lysis buffer containing 8 M carbamide (Gibco; Thermo Fisher Scientific, Inc.), 30 mM HEPES (Wuhan Boster Biological Technology, Ltd.), 1 mM PMSF (Amresco, LLC), 2 mM EDTA (Amresco, LLC), and 10 mM DTT (Promega Corporation) was added to cells and centrifuged at 20,000 x g and 4˚C for 30 min to collect the supernatant. Protein concentrations were determined using the Bradford method. For digestion, each sample was reduced with 10 mM dithiothreitol for 60 min at 56˚C and alkylated using 55 mM iodoacetamide for 60 min at room temperature in the dark. The proteins were digested with 1 μg/μl trypsin at a weight ratio of 1:30 (trypsin:protein) overnight at 37˚C. Tryptic peptides were lyophilized and resuspended in 0.5 M Triethylammonium bicarbonate. Following trypsin digestion, each iTRAQ reagent was dissolved in isopropanol and added to the appropriate peptide mixture. A total of 3 biological replicates of the ET group were labelled with iTRAQ tags 113, 114 and 115, respectively. Similarly, 3 biological replicates of the LPS group were labelled with iTRAQ tags 118, 117 and 116, respectively. The labelled peptide mixtures were incubated at room temperature for 2 h and obtained by vacuum-drying. Then, peptides were desalted using a Strata X C18 SPE column (Phenomenex, Torrance, CA, USA), and analyzed using a mass spectrometer (TripleTOF 6600; SCIEX, Framingham, MA, USA). The instrument parameters were as follows: Mass range, 350-2,000 m/z for time-of-flight mass spectrometry (TOF MS) and 100-1,500 m/z for TOF MS/MS; dynamic exclusion, 12.0 sec. Mass spectra raw data were analyzed with ProteinPilotä software (version 5.0; SCIEX). The parameters for the analysis were set as follows: Cys alkylation, iodoacetamide; digestion, trypsin; species, *Mus musculus*. Peptides were identified using a false discovery rate of <1%. Proteins were considered differentially expressed if they differed in at least 2 of the 3 biological replicates. The criteria of $P<0.05$ and fold change (ET/LPS)>1.2 or <0.833 were selected to identify up- and down-regulated proteins.

Bioinformatics analysis. Functional enrichment analysis for the differentially expressed proteins was performed using the Database for Annotation, Visualization and Integrated Discovery (DAVID version 6.7; david.ncifcrf.gov) for Gene Ontology annotation and Kyoto Encyclopedia of Genes and Genomes (KEGG; www.genome.jp/kegg/) pathway analysis. $P<0.05$ was selected as the cut-off criterion. A protein-protein interaction network was constructed using the inBio Map database (www.intomics.com/inbio/map). Key genes located in the center of the network were subsequently verified.

Western blot analysis. Cell lysates were obtained using a lysis buffer containing phosphatase inhibitor and the protease inhibitor phenylmethanesulfonyl fluoride (100 mM; cat. no. KGP250; Nanjing KeyGen Biotech Co., Ltd.) and the protein concentration in the lysates determined by Bradford assay. A total of 100 μg lysate was separated by 10% SDS-PAGE and then transferred to a polyvinylidene difluoride (PVDF) membrane at 250 mA for 1 h. The PVDF membranes were blocked with 5% FBS for 1.5 h at 37˚C and incubated overnight at 4˚C with rabbit anti-mouse antibodies against high mobility group (HMG)A1 (1:10,000; cat. no. ab129153; Abcam), HMGA2 (1:1,000; cat. no. D1A7; Cell Signaling Technology, Inc.), HMGB1 (1:10,000; cat. no. ab79823; Abcam), HMGB2 (1:10,000; cat. no. ab124670; Abcam) and β-actin (1:1,000; cat. no. BM0627; Wuhan Boster Biological Technology, Ltd.). The PVDF membranes were washed three

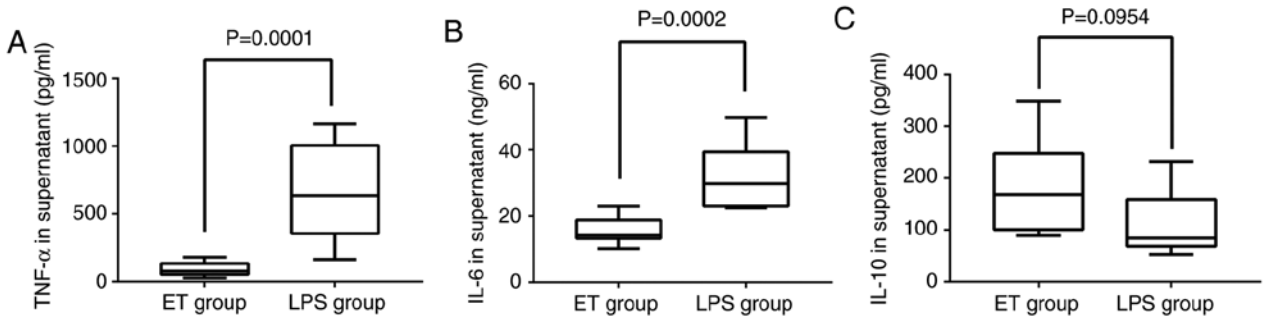

Figure 1. Concentration of TNF-α, IL-6 and IL-10 in the 2 groups as detected by ELISA. Following stimulation with high-dose LPS (100 ng/ml) for 4 h, (A) the level of TNF-α in the supernatant of the ET group (18,273.5±101,54.4 pg/ml) was lower compared with that in the LPS group (133,233.7±689, 55.9 pg/ml) and (B) the level of IL-6 in the supernatant of the ET group (1,549.8±399.2 pg/ml) was lower compared with that in the LPS group (3,175.8±959.0 pg/ml). (C) The level of IL-10 in the supernatant of the ET group (351.1±184.2 pg/ml) was higher when compared the LPS group (220.3±121.4 pg/ml), but the difference was not statistically significant. LPS, lipopolysaccharide; ET, endotoxin tolerance; IL, interleukin; TNF, tumor necrosis factor.

times with TBST (0.1% Tween) and incubated with goat anti-rabbit Immunoglobulin G-HRP (1:1,000; cat. no. BA1054; Wuhan Boster Biological Technology, Ltd.) for 1.5 h at 37˚C, followed by the 3,3'-diaminobenzidine (EMD Millipore) method at room temperature for 15 sec. PVDF membranes were subjected to densitometry analysis (chemiDox.XRS+; Bio-Rad Laboratories, Inc.), then the image was analyzed using Quantity One 4.0 software (Bio-Rad Laboratories, Inc.).

Statistical analysis. Data are expressed as the mean ± standard error of the mean. SPSS version 21.0 (IBM Corp., Armonk, NY, USA) was used for data analysis. Statistical analysis was performed using an independent sample Student's t-test. P<0.05 was considered to indicate a statistically significant difference.

Results

Different concentrations of TNF-α, IL-6 and IL-10 between the ET and LPS groups. To determine the concentrations of cytokines in the ET and LPS groups, the supernatants of the cells were analyzed by ELISA. As indicated in Fig. 1A and B, TNF-α and IL-6 were significantly downregulated in the ET group when compared with the LPS group (P<0.05). The expression of IL-10 in the ET group was higher when compared with in the LPS group, but the difference was not statistically significant (P>0.05; Fig. 1C). These results indicated that the ET model had been successfully constructed.

Expression of CD16/32 on the cell surface in the ET and LPS groups. CD16/32 is the cell surface marker that is induced in M1-polarized cells. Based on the theory that ET skews cell polarization into an M2-like phenotype, and the number of M1-polarized cells will not continue to increase (8), cell surface marker analysis was performed to determine the expression level of CD16/32 by flow cytometry. As shown in Fig. 2, following stimulation with high-dose LPS for 4 h , CD16/32 was induced in the ET group compared with the LPS group or untreated sample (P<0.05; Fig. 2C and D), but following stimulation with LPS for 24 h, significant downregulation of this marker was observed in the ET group compared with the LPS group (P<0.05; Fig. 2E and F). The results indicated that there were more M1-polarized cells in the ET group compared with in the LPS group at the early stage (4 h), and the ET model was successfully constructed.

iTRAQ analysis of differentially expressed proteins. A total of 3 biological replicates were performed for the ET and LPS groups (n=3). A total of 235 different proteins were identified by iTRAQ, and there were 63 differentially expressed proteins identified in at least 2 of the experiments. Of the 63 differentially expressed proteins, 36 upregulated proteins with >1.2-fold difference and 27 downregulated proteins with <0.833-fold difference were selected between the ET and LPS groups (Fig. 3). Specific upregulated proteins are presented in Table I and downregulated proteins are presented in Table II.

Functional enrichment analysis and pathway annotation of differentially expressed proteins. The 63 differentially expressed proteins were analyzed by DAVID to study their biological processes, molecular functions and cellular component. The biological processes of these proteins were mainly involved in the growth and development of organ tissues, the regulation of biological quality and responses to external stimuli (Fig. 4). The molecular functions analysis demonstrated that these proteins were mainly involved in 'oxidoreductase activation', 'receptor binding', 'DNA binding' and 'antioxidant activity' (Fig. 5). In the cellular component analysis, the differentially expressed proteins were mainly located in 'chromatin', the 'extracellular space', 'membrane-bounded vesicles' and 'cytoplasmic vesicles' (Fig. 6). According to KEGG pathway analysis, the 63 differentially expressed proteins were involved in 27 signaling pathways (P<0.05). The top 10 signaling pathways included TLR signaling pathway, nuclear factor (NF)-κB signaling pathway, TNF signaling pathway and antigen presentation processes (Table III).

Protein-protein interaction analysis. The inBio Map database was used to construct a protein-protein interaction network (Fig. 7). From the 63 differential proteins, 4 key proteins were located at the core of network. According to the bioinformatics analysis, HMGA1/2 and HMGB1/2 were selected for further study.

Validation of the key proteins HMGA1, HMGA2, HMGB1 and HMGB2. To validate the 4 key proteins, western blot analysis

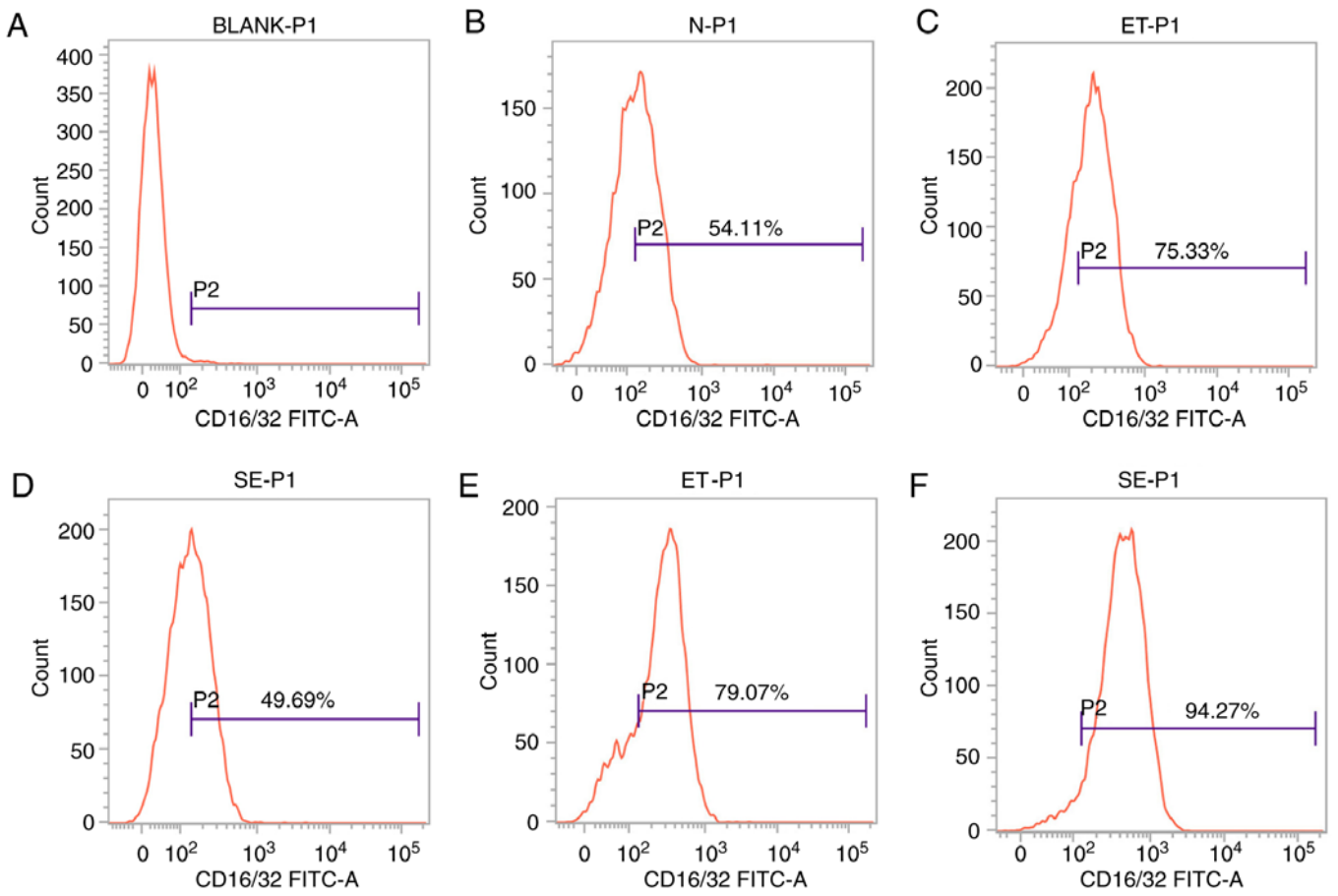

Figure 2. Expression of CD16/32 on the cell surface in the ET and LPS groups. The cell surface marker CD16/32 was analyzed by flow cytometry. (A) BLANK-P1: Isotype staining; (B) N-P1: No staining; (C) ET-P1: ET group following treatment with high-dose LPS for 4 h; (D) SE-P1: LPS group following treatment with high-dose LPS for 4 h; (E) ET-P1: ET group following treatment with high-dose LPS for 24 h; (F) SE-P1: LPS group following treatment with high-dose LPS for 24 h. The positive rate of CD16/32 in the ET group (75.33%) was higher compared with the LPS group (49.69%) following stimulation with high-dose LPS for 4 h ($P<0.05$). Following treatment for 24 h, the positive rate of CD16/32 (79.07%) in the ET group was lower when compared with the LPS group (94.27%; $P<0.05$). LPS, lipopolysaccharide; ET, endotoxin tolerance; CD, cluster of differentiation; FITC, fluorescein isothiocyanate; N, no staining; ET, endotoxin tolerance; SE, sepsis.

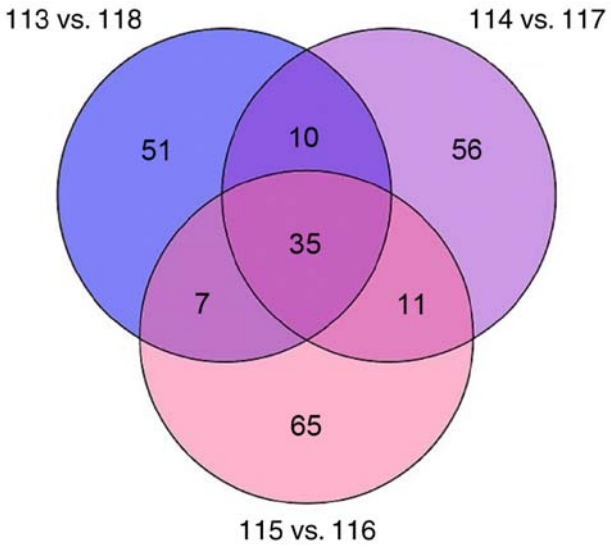

Figure 3. Differentially expressed proteins between the ET and LPS groups. A total of 63 differentially expressed proteins were identified by isobaric tags for relative and absolute quantitation in 2 of the 3 repeated experiments. LPS, lipopolysaccharide; ET, endotoxin tolerance.

was performed. The expression of HMGA1 and HMGA2 in the ET group was higher compared with the LPS group at 4 h following high-dose LPS stimulation, while HMGB1 and HMGB2 exhibited the opposite trend in expression under the same conditions (Fig. 8). These results were consistent with the findings from iTRAQ analysis.

Discussion

Sepsis is a systemic infection caused by various other infections. It can develop into septic shock and multiple organ failure, with a high mortality rate (18). The pathophysiological changes of sepsis result from multifactorial interactions. Fortunately, the discovery of the phenomenon of ET provides a new avenue for identifying treatments for sepsis. Paul Beeson (19) initially identified ET and demonstrated that repeated injections of the typhoid bacilli vaccine in rabbits significantly reduced the fever caused by the vaccine. ET has been observed in infection, and certain studies have demonstrated that ET is associated with innate immunity (5), while monocyte macrophages are an important part of innate immunity (20). Large differences in

Table I. The 36 upregulated proteins in the present study.

Number	Code no.	Symbol	Name	Ratio
1	P10923	Spp1	Osteopontin	2.168
2	P52927	Hmga2	High mobility group protein HMGI-C	1.907
3	P25085	Il1rn	Interleukin-1 receptor antagonist protein	1.854
4	Q07797	Lgals3bp	Galectin-3-binding protein	1.843
5	Q64339	Isg15	Ubiquitin-like protein ISG15	1.832
6	P54987	Acod1	Cis-aconitate decarboxylase	1.641
7	P09671	Sod2	Superoxide dismutase [Mn], mitochondrial	1.641
8	Q05769	Ptgs2	Prostaglandin G/H synthase 2	1.617
9	Q99JT1	Gatb	Glutamyl-tRNA(Gln) amidotransferase subunit B, mitochondrial	1.531
10	P99029	Prdx5	Peroxiredoxin-5, mitochondrial	1.489
11	Q05816	Fabp5	Fatty acid-binding protein, epidermal	1.474
12	P27046	Man2a1	α-mannosidase 2	1.447
13	P37040	Por	NADPH-cytochrome P450 reductase	1.444
14	P45377	Akr1b8	Aldose reductase-related protein 2	1.415
15	P30204	Msr1	Macrophage scavenger receptor types I and II	1.402
16	P35700	Prdx1	Peroxiredoxin-1	1.396
17	P10855	Ccl3	C-C motif chemokine 3	1.386
18	P20029	Hspa5	78 kDa glucose-regulated protein	1.375
19	P17095	Hmga1	High mobility group protein HMG-I/HMG-Y	1.363
20	Q9Z0J0	Npc2	Epididymal secretory protein E1	1.362
21	Q9JHK5	Plek	Pleckstrin	1.336
22	E9Q555	Rnf213	E3 ubiquitin-protein ligase RNF213	1.328
23	D0QMC3	Mndal	Myeloid cell nuclear differentiation antigen-like protein	1.327
24	P20108	Prdx3	Thioredoxin-dependent peroxide reductase, mitochondrial	1.304
25	P97429	Anxa4	Annexin A4	1.298
26	P01902	H2-K1	H-2 class I histocompatibility antigen, K-D alpha chain	1.282
27	Q8BLN5	Lss	Lanosterol synthase	1.279
28	P47758	Srprb	Signal recognition particle receptor subunit β	1.276
29	O35215	Ddt	D-dopachrome decarboxylase	1.269
30	P10852	Slc3a2	4F2 cell-surface antigen heavy chain	1.261
31	Q9WVK4	Ehd1	EH domain-containing protein 1	1.253
32	Q8BSY0	Asph	Aspartyl/asparaginyl β-hydroxylase	1.249
33	Q9QUJ7	Acsl4	Long-chain-fatty-acid-CoA ligase 4	1.247
34	P53395	Dbt	Lipoamide acyltransferase component of branched-chain α-keto acid dehydrogenase complex, mitochondrial	1.237
35	P61620	Sec61a1	Protein transport protein Sec61 subunit α isoform 1	1.221
36	Q6NZF1	Zc3h11a	Zinc finger CCCH domain-containing protein 11A	1.208

Proteins were identified by isobaric tags for relative and absolute quantitation as having >1.2-fold differences in their expression level between the lipopolysaccharide and endotoxin tolerance groups.

gene expression were analyzed by microarray analysis during ET and the ETS family of transcription factors were the most associated with ET (9). In the present study, an ET model was constructed using 2 doses of LPS, and verified by measuring the concentration of TNF-α and IL-6, and the proportion of cells with the M1-like phenotype.

Proteomics is the study of the expression of all proteins in cells and tissues at specific times and spatial distributions. iTRAQ technology, a novel high-throughput MS method, is a labeling technique for peptides using isotopes *in vitro*. The specific quantitative information of the protein is collected by specifically labeling the amino group of the polypeptide and then performing MS analysis (21). iTRAQ is a commonly used high-channel screening technique, and has been used to study the proteomics of sepsis in recent years (22,23). In the present study, iTRAQ technology was used to screen for differentially expressed proteins between ET and sepsis, and 63 differentially expressed proteins were selected.

Bioinformatics enables the analysis of large-scale genetic, protein, metabolite and other biomolecular data by

Table II. The 27 downregulated proteins in the present study.

Number	Code number	Symbol	Name	Ratio
1	P57759	Erp29	Endoplasmic reticulum resident protein 29	0.827
2	Q61093	Cybb	Cytochrome b-245 heavy chain	0.822
3	Q9ESY9	Ifi30	Gamma-interferon-inducible lysosomal thiol reductase	0.821
4	P14152	Mdh1	Malate dehydrogenase, cytoplasmic	0.818
5	P17742	Ppia	Peptidyl-prolyl cis-trans isomerase A	0.811
6	Q09014	Ncf1	Neutrophil cytosol factor 1	0.807
7	Q04447	Ckb	Creatine kinase B-type	0.799
8	Q9Z1B5	Mad2l1	Mitotic spindle assembly checkpoint protein MAD2A	0.791
9	P43274	Hist1h1e	Histone H1.4	0.789
10	P20060	Hexb	Beta-hexosaminidase subunit β	0.786
11	P16110	Lgals3	Galectin-3	0.761
12	P54227	Stmn1	Stathmin	0.758
13	P63158	Hmgb1	High mobility group protein B1	0.757
14	P23198	Cbx3	Chromobox protein homolog 3	0.748
15	P43276	Hist1h1b	Histone H1.5	0.726
16	P10749	Il1b	Interleukin-1β	0.725
17	P43275	Hist1h1a	Histone H1.1	0.721
18	P30681	Hmgb2	High mobility group protein B2	0.714
19	P62806	Hist1h4a	Histone H4	0.702
20	P06804	Tnf	Tumor necrosis factor	0.701
21	Q91YS8	Camk1	Calcium/calmodulin-dependent protein kinase type 1	0.692
22	P07091	S100a4	Protein S100-A4	0.681
23	Q91VW3	Sh3bgrl3	SH3 domain-binding glutamic acid-rich- like protein 3	0.679
24	P20065-2	Tmsb4x	Isoform Short of Thymosin β-4	0.676
25	P63254	Crip1	Cysteine-rich protein 1	0.657
26	P15864	Hist1h1c	Histone H1.2	0.615
27	O54962	Banf1	Barrier-to-autointegration factor	0.590

Proteins with <0.833-fold differential expression between the lipopolysaccharide and endotoxin tolerance groups were identified using isobaric tags for relative and absolute quantitation.

Table III. Top 10 signaling pathways analyzed by Kyoto Encyclopedia of Genes and Genomes pathway analysis.

Path number	Pathway name	P-value	Number of proteins
mmu05332	Graft-versus-host disease	<0.0001	3
mmu04940	Type I diabetes mellitus	0.0001	3
mmu04612	Antigen processing and presentation	0.0007	4
mmu04060	Cytokine-cytokine receptor interaction	0.0011	3
mmu03060	Protein export	0.0017	3
mmu04620	Toll-like receptor signaling pathway	0.0031	4
mmu04064	NF-κB signaling pathway	0.0137	3
mmu05206	MicroRNAs in cancer	0.0246	3
mmu04668	TNF signaling pathway	0.0246	3
mmu03320	PPAR signaling pathway	0.0338	2

The 63 differentially expressed proteins were mainly involved in 27 signaling pathways (P<0.05); the top 10 signaling pathways are presented.

the application of information science (24). The biological processes of the 63 differentially expressed proteins were mainly involved in the growth and development of organ tissues, the regulation of biological quality and response to external stimuli, which indicated that the differential proteins had extensive biological functions in the ET state. In the present

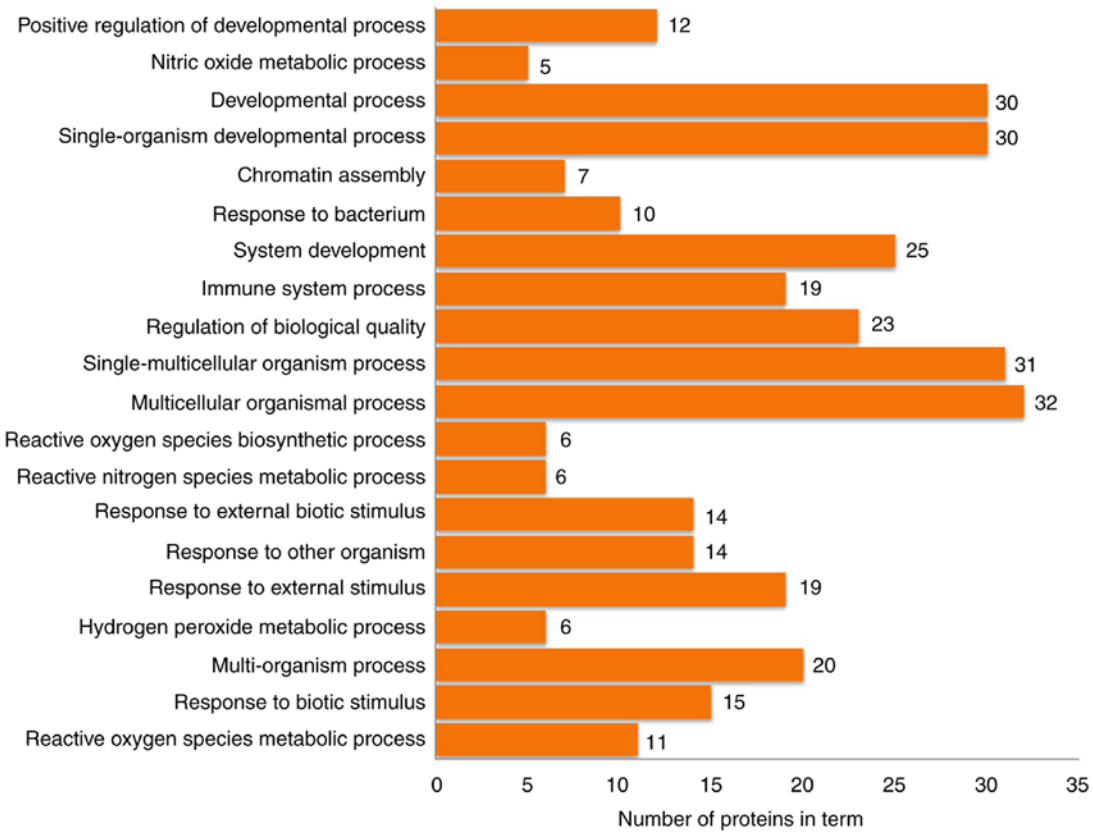

Figure 4. Biological process terms identified by functional enrichment analysis.

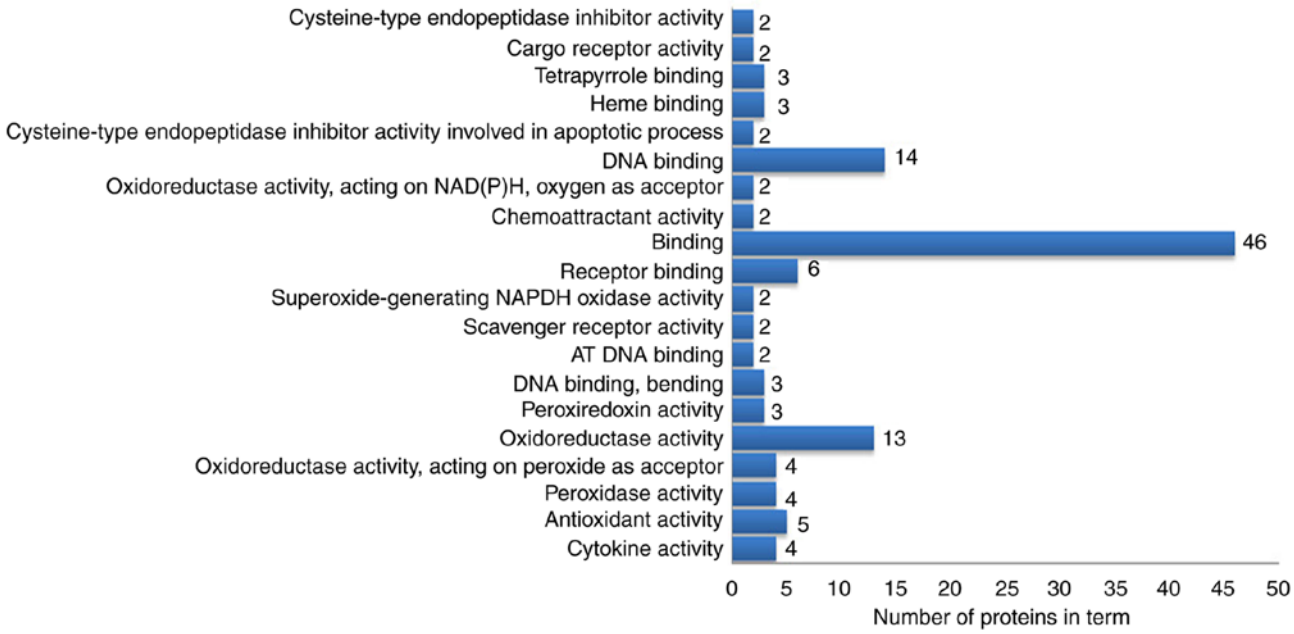

Figure 5. Molecular function terms identified by functional enrichment analysis.

study, differential proteins were involved in 27 signaling pathways, including the TLR, NF-κB and TNF signaling pathways, and antigen presentation processes. In ET, the TLR and the NF-κB signaling pathways were inhibited (5,24), and the downstream effector factor, TNF-α, was downregulated. The results of the present study are consistent with these previous findings.

The levels of HMGA1 and HMGA2 in the ET group were higher compared with those in the LPS group, while HMGB1 and HMGB2 exhibited the opposite trend in the present study. Previous studies have identified that HMGB1 expression is downregulated during ET and reduces inflammatory damage (25), which is associated with the JAK/STAT1 signaling

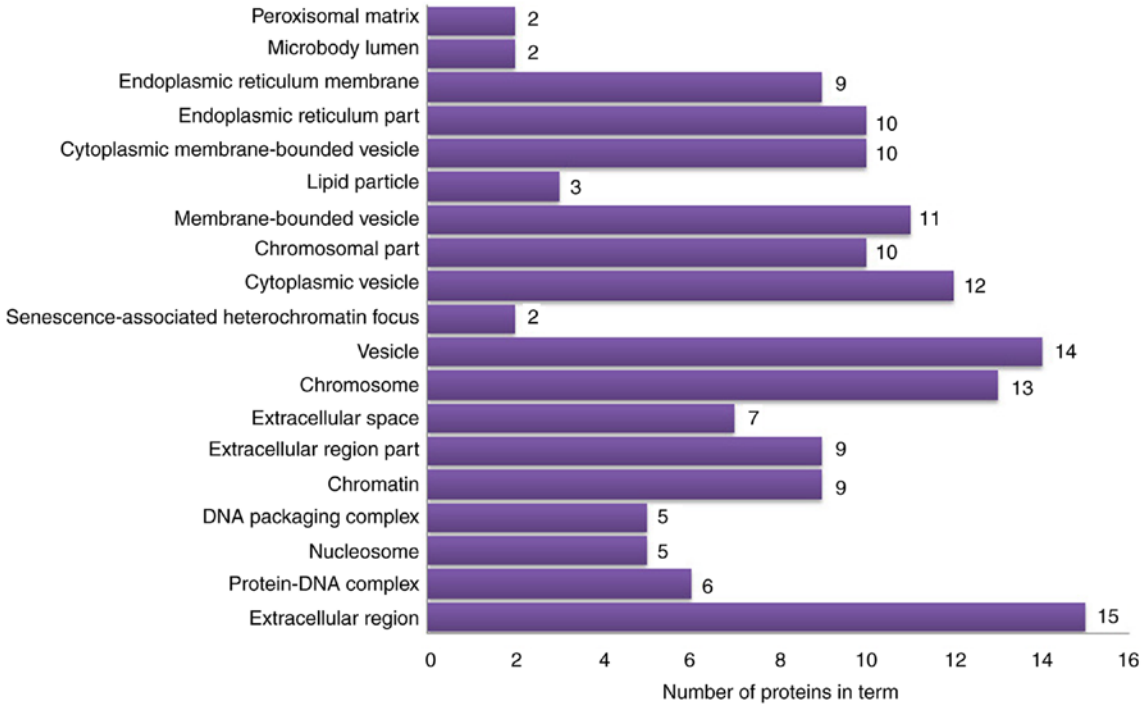

Figure 6. Cellular component terms identified by functional enrichment analysis.

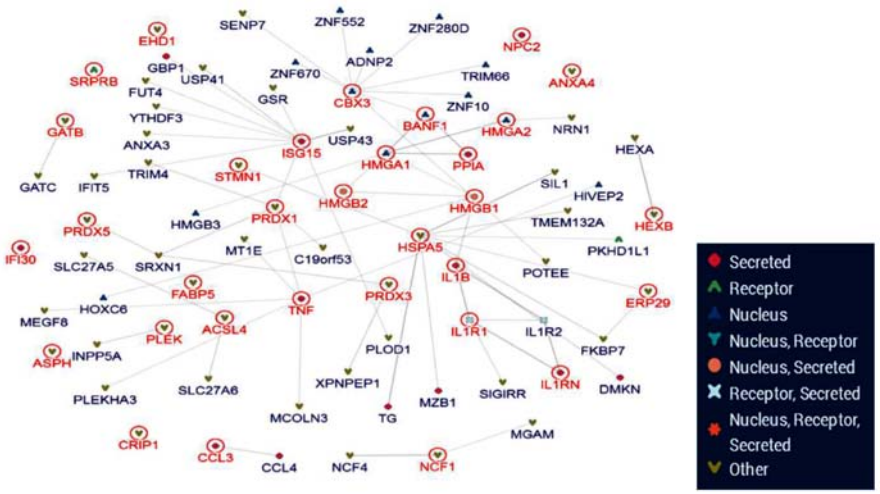

Figure 7. Protein-protein interaction network. The inBio Map database was used to construct the protein-protein interaction network. HMGA1/2 and HMGB1/2 proteins were located at the core of the network. HMG, high mobility group.

pathway (26). As a late mediator of sepsis, HMGB1 is released into the extracellular space by activated macrophages ~20 h after endotoxin stimulation *in vivo* and *in vitro* (27). The present study also demonstrated that HMGA1, HMGA2 and HMGB2 may be involved in the formation of ET. The association between these 4 proteins in the formation of ET remains unclear. The reasons for this phenomenon may involve the following 2 mechanisms: Firstly, there may be a competitive relationship between the 4 proteins for the development of ET and sepsis; secondly, they may serve a phased role in ET at different times.

In conclusion, proteomics combined with bioinformatics were applied to explore the mechanism of ET. In the present study, HMGA1/2 and HMGB1/2 exhibited opposite expression trends in ET, and the specific interactions between them

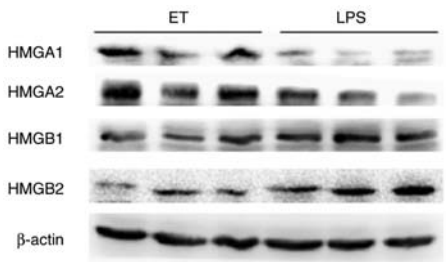

Figure 8. Validation of HMGA1, HMGA2, HMGB1 and HMGB2 by western blot analysis. The expression of HMGA1 and HMGA2 in the ET group was higher compared with the LPS group at 4 h after high-dose LPS stimulation), while HMGB1 and HMGB2 exhibited the opposite expression trend under the same conditions. LPS, lipopolysaccharide; ET, endotoxin tolerance; HMG, high mobility group.

requires further study. iTRAQ technology can be used to screen differentially expressed proteins, but it is costly and only suitable for a small number of samples. Therefore, it must be used in combination with other molecular biological techniques.

Acknowledgements

The authors would like to thank MD Xiaoping Tang (Experimental Medicine Center, The Affiliated Hospital of Southwest Medical University, Luzhou, Sichuan 646000, China) for Flow cytometric technical support.

Funding

The present study was funded by grants from Southwest Medical University, China (grant no. 2015YJ-091) and the Affiliated Hospital of Southwest Medical University, China (grant no. 2015-PT-015).

Availability of data and materials

All data generated or analyzed during the present study are included in this published article.

Authors' contributions

QZ contributed to study design, drafted the manuscript and gave final approval of the manuscript; YCH contributed to study design and data analysis, and gave final approval of the manuscript; JZ contributed to experimental operation and gave final approval of the manuscript; CLD acquired the data, revised the manuscript for important intellectual content, gave final approval of the version to be published, and agreed to be accountable for all aspects of the work.

Ethics approval and consent to participate

Not applicable.

Patient consent for publication

Not applicable.

Competing interests

The authors declare that they have no competing interests.

References

1. Taeb AM, Hooper MH and Marik PE: Sepsis: Current definition, pathophysiology, diagnosis, and management. Nutr Clin Pract 32: 296-308, 2017.
2. Dellinger RP, Levy MM, Rhodes A, Annane D, Gerlach H, Opal SM, Sevransky JE, Sprung CL, Douglas IS, Jaeschke R, *et al*: Surviving sepsis campaign: International guidelines for management of severe sepsis and septic shock, 2012. Crit Care Med 41: 580-637, 2013.
3. Salomao R, Brunialti MK, Rapozo MM, Baggio-Zappia GL, Galanos C and Freudenberg M: Bacterial sensing, cell signaling, and modulation of the immune response during sepsis. Shock 38: 227-242, 2012.
4. Bai Y, Lu B and Sun Q: Pre-exposure to fine particulate matters may induce endotoxin tolerance in a mouse model. Austin J Environ Toxicol 1: 1004, 2015.
5. López-Collazo E and Del Fresno C: Pathophysiology of endotoxin tolerance: Mechanisms and clinical consequences. Crit Care 17: 242, 2013.
6. Biswas SK and Lopez-Collazo E: Endotoxin tolerance: New mechanisms, molecules and clinical significance. Trends Immunol 30: 475-487, 2009.
7. Lacatus M: Innate immunity in surgical patients. Chirurgia (Bucur) 108: 18-25, 2013.
8. Draisma A, Pickkers P, Bouw MP and van der Hoeven JG: Development of endotoxin tolerance in humans in vivo. Crit Care Med 37: 1261-1267, 2009.
9. Pena OM, Pistolic J, Raj D, Fjell CD and Hancock RE: Endotoxin tolerance represents a distinctive state of alternative polarization (M2) in human mononuclear cells. J Immunol 186: 7243-7254, 2011.
10. Milot E, Fotouhi-Ardakani N and Filep JG: Myeloid nuclear differentiation antigen, neutrophil apoptosis and sepsis. Front Immunol 3: 397, 2012.
11. Xiong Y and Medvedev AE: Induction of endotoxin tolerance in vivo inhibits activation of IRAK4 and increases negative regulato rs IRAK-M, SHIP-1, and A20. J Leukoc Biol 90: 1141-1148, 2011.
12. Piao W, Song C, Chen H, Diaz MA, Wahl LM, Fitzgerald KA, Li L and Medvedev AE: Endotoxin tolerance dysregulates MyD88- and Toll/IL-1R domain-containing adapter inducing IFN-beta-dependent pathways and increases expression of negative regulators of TLR signaling. J Leukoc Biol 86: 863-875, 2009.
13. Cohen P: The search for physiological substrates of MAP and SAP kinases in mammalian cells. Trends Cell Biol 7: 353-361, 1997.
14. Nahid MA, Satoh M and Chan EK: MicroRNA in TLR signaling and endotoxin tolerance. Cell Mol Immunol 8: 388-403, 2011.
15. Nahid MA, Satoh M and Chan EK: Interleukin 1β-responsive MicroRNA-146a is critical for the cytokine-induced tolerance and cross-tole rance to toll-like receptor ligands. J Innate Immun 7: 428-440, 2015.
16. Curtale G, Mirolo M, Renzi TA, Rossato M, Bazzoni F and Locati M: Negative regulation of Toll-like receptor 4 signaling by IL-10-dependent microRNA-146b. Proc Natl Acad Sci U S A 110: 11499-11504, 2013.
17. Liu M, John CM and Jarvis GA: Induction of endotoxin tolerance by pathogenic neisseria is correlated with the inflammatory potentia l of lipooligosaccharides and regulated by microRNA-146a. J Immunol 192: 1768-1777, 2014.
18. Pena OM, Hancock DG, Lyle NH, Linder A, Russell JA, Xia J, Fjell CD, Boyd JH and Hancock RE: An endotoxin tolerance signature predicts sepsis and organ dysfunction at initial clinical presentati on. EBioMedicine 1: 64-71, 2014.
19. Beeson PB: Development of tolerance to typhoid bacterial pyrogen and its abolition by reticulo-endothelial blockade. Proc Soc Exp Biol Med 61: 248-250, 1946.
20. Morris MC, Gilliam EA and Li L: Innate immune programing by endotoxin and its pathological consequences. Front Immunol 5: 680, 2015.
21. Rauniyar N and Yates JR 3rd: Isobaric labeling-based relative quantification in shotgun proteomics. J Proteome Res 13: 5293-5309, 2014.
22. Cao Z, Yende S, Kellum JA, Angus DC and Robinson RA: Proteomics reveals age-related differences in the host immune response to sepsis. J Proteome Res 13: 422-432, 2014.
23. Wu Z, Pan D, Guo Y, Zeng X and Sun Y: iTRAQ proteomic analysis of N-acetylmuramic acid mediated anti-inflammatory capacity in LPS-induced R AW 264.7 cells. Proteomics 15: 2211-2219, 2015.
24. Yang YX and Li L: Identification of potential biomarkers of sepsis using bioinformatics analysis. Exp Ther Med 13: 1689-1696, 2017.
25. Li S, Luo C, Yin C, Peng C, Han R, Zhou J, He Q and Zhou J: Endogenous HMGB1 is required in endotoxin tolerance. J Surg Res 185: 319-328, 2013.
26. Yang NB, Ni SL, Li SS, Zhang SN, Hu DP and Lu MQ: Endotoxin tolerance alleviates experimental acute liver failure via inhibition of high mobility group box 1. Int J Clin Exp Pathol 8: 9062-9071, 2015.
27. Wang H, Liao H, Ochani M, Justiniani M, Lin X, Yang L, Al-Abed Y, Wang H, Metz C, Miller EJ, *et al*: Cholinergic agonists inhibit HMGB1 release and improve survival in experimental sepsis. Nat Med 10: 1216-1221, 2004.